Solution of large deformation contact problems with friction between Blatz-Ko hyperelastic bodies

Zhi-Qiang Feng, François Peyraut, Nadia Labed

Solution of large deformation contact problems with friction between Blatz–Ko hyperelastic bodies

Zhi-Qiang Feng [a,*], François Peyraut [b], Nadia Labed [b]

[a]Laboratoire de Mécanique d'Evry, EA3332, Université d'Evry-Val d'Essonne, Laboratoire CEMIF, IUP, 40,rue du Pelvoux, 91020 Evry cedex, France

[b]Laboratoire Mécatronique 3M, University de Technologie de Belfort-Montbeeliard Rue du Château, Sévenans, 90010 Belfort cedex, France

The present paper is devoted to the analysis of the contact problems with Coulomb friction and large deformation between two hyperelastic bodies. One approach to separate the material nonlinearity and contact nonlinearity is presented. The total Lagrangian formulation is adopted to describe the geometrically nonlinear behavior. Nondifferentiable contact potentials are regularized by means of the augmented Lagrangian method. Numerical examples are carried out in two cases: rigid–deformable contact and deformable–deformable contact with large slips. The numerical results prove that the proposed approach is robust and efficient concerning numerical stability.

Keywords: Contact and friction; Hyperelastic large deformation; Finite element

1. Introduction

The analysis of contact problems with friction is of great importance in many engineering applications. The numerical treatment of the unilateral contact with dry friction is certainly one of the nonsmooth mechanics topics for which many efforts have been made in the past. In the literature, many attempts have been developed to deal with such problems using the finite element method, these include the penalty function method [1–4], the flexibility method [5,6], the mathematical programming method [7–9], the Lagrangian multiplier method [10,11] and the augmented

* Corresponding author. Tel.: +33-1-69-47-75-01; fax: +33-1-69-47-75-99.
E-mail address: feng@iup.univ-evry.fr (Z.-Q. Feng).

Lagrangian method [12–17]. A large literature base is available for a variety of numerical algorithms [18,19]. To the author's best knowledge, however, numerical modeling of frictional contact problems between hyperelastic bodies undergoing large deformations remains limited. A continuum framework for finite element discretization of large displacement contact is presented by Curnier et al. [20,21] and by Klarbring [22]. Recently, analytical investigations on the contact problems between two homogeneous and isotropic soft bodies were performed to simulate the contact of human buttocks and seat cushions [23]. An existence result of frictionless contact problem between a hyperelastic body and a rigid plane has been obtained by Bretelle et al. [24]. However, no applications were presented. In the present work, the intention is to present numerical investigations on the frictional contact problems between hyperelatic bodies with large deformations and large slips. Two numerical examples are performed in this study to show the validity of the developed models.

2. Modeling of contact problems in a reduced system

In this section, the geometric and kinematic quantities found suitable for describing the contact compatibility of deformable bodies are defined and the local algorithm for contact modeling is presented.

2.1. Contact kinematics

First of all, some basic definitions and notations are set up. For the sake of simplicity, let us consider contact between two bodies Ω_1 and Ω_2, one of which may be a rigid foundation. In order to state the contact constraints, we have to find the minimum distance of a point P of one body with respect to the other one. The displacements of the particles of Ω_1 and Ω_2 being respectively $\mathbf{u}_1$ and $\mathbf{u}_2$, the relative displacement is: $\mathbf{u} = \mathbf{u}_1 - \mathbf{u}_2$. Let $\mathbf{r}$ be the contact traction acting at P from Ω_2 onto Ω_1. Then Ω_2 is subjected to the traction $-\mathbf{r}$, acting from Ω_1. Let $\mathbf{n}$ denote the normal unit vector at the projection point P' to the bodies, directed towards Ω_1, and $\mathbf{T}(t_1, t_2)$ denotes the orthogonal plane to $\mathbf{n}$ in $\mathbf{R}^3$ (Fig. 1).

Any element $\mathbf{u}$ and $\mathbf{r}$ may uniquely be decomposed in the form:

$$\begin{aligned} &\mathbf{u} = \mathbf{u}_t + u_n\mathbf{n}, \quad \mathbf{u}_t \in \mathbf{T}, \quad u_n \in \mathbf{R} \\ &\mathbf{r} = \mathbf{r}_t + r_n\mathbf{n}, \quad \mathbf{r}_t \in \mathbf{T}, \quad r_n \in \mathbf{R} \end{aligned} \tag{1}$$

Classically, a unilateral contact law is characterized by a geometric condition of nonpenetration, a static condition of no-adhesion and a mechanical complementarity condition. These three

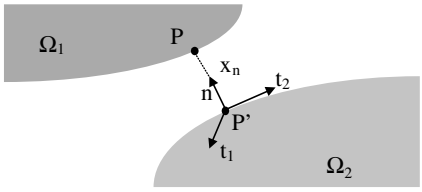

Fig. 1. Projection and gap vector.

conditions are so-called Signorini conditions written in terms of the signed contact distance x_n and the normal contact force r_n:

$$x_n \geqslant 0; \quad r_n \geqslant 0 \text{ and } r_n x_n = 0 \tag{2}$$

where x_n denotes the magnitude of the gap between the contact node and the target surface and is a violation of the contact compatibility.

$$x_n = g + u_n \tag{3}$$

with the initial gap:

$$g = (\mathbf{x}_1 - \mathbf{x}_2) \cdot \mathbf{n} \tag{4}$$

Classically, a rate independent dry friction law is characterized by a kinematic slip rule. Let K_μ denote Coulomb's cone:

$$K_\mu = \{\mathbf{r} \in \mathbf{R}^3 \text{ such that } |\mathbf{r}_t| \leqslant \mu r_n\} \tag{5}$$

The complete contact law is a complex nonsmooth dissipative law including three statuses: no contact, contact with sticking and contact with sliding. The resulting analytical transcripts yields two overlapped "if...then...else" statements:

$$\begin{aligned} &\text{if } r_n = 0 \text{ then } x_n \geqslant 0 \quad \text{! no contact} \\ &\text{else if } \mathbf{r} \in K_\mu \text{ then } \mathbf{u} = 0 \quad \text{! sticking} \\ &\text{else } (r_n > 0 \text{ and } \mathbf{r} \in K_\mu), \quad \left\{ x_n = 0 \text{ and } \exists \lambda > 0 \text{ such that } |u_t| = -\lambda \frac{\mathbf{r}_t}{|\mathbf{r}_t|} \right\} \quad \text{! sliding} \end{aligned} \tag{6}$$

An alternative statement is the inverse law:

$$\begin{aligned} &\text{if } x_n > 0 \text{ then } \mathbf{r} = 0 \quad \text{! no contact} \\ &\text{else if } \mathbf{u} = 0 \text{ then } \mathbf{r} \in K_\mu \quad \text{! sticking} \\ &\text{else } \mathbf{u} \in \mathbf{T}, \ r_n > 0 \text{ and } \mathbf{r}_t = -\mu r_n \frac{\mathbf{u}_t}{|\mathbf{u}_t|} \quad \text{! sliding} \end{aligned} \tag{7}$$

From convex analysis, the above contact and friction laws are equivalent to the following variational inequality [25]:

Find $(\mathbf{r}_t, r_n) \in K_\mu$ such that

$$(x_n - \mu|\hat{\mathbf{u}}_t|)(r_n^* - r_n) + \hat{\mathbf{u}}_t \cdot (\mathbf{r}_t^* - \mathbf{r}_t) \leqslant 0 \quad \forall (\mathbf{r}_t^*, r_n^*) \in K_\mu \tag{8}$$

where

$$\hat{\mathbf{u}}_t = \lambda \frac{\mathbf{r}_t}{|\mathbf{r}_t|} \quad \text{for some } \lambda = 0$$

2.2. Local algorithm

In order to avoid nondifferentiable potentials that occur in nonlinear mechanics, such as in contact problems, it is convenient to use the Augmented Lagrangian Method [14–17]. This method, applied to the variational inequality (8), leads to the following implicit equation

$$\mathbf{r} = \mathrm{proj}((r_n + \rho_n(x_n - \mu|\hat{\mathbf{u}}_t|), \mathbf{r}_t + \rho_t \mathbf{u}_t), K_\mu) \tag{9}$$

where ρ_n and ρ_t are real positive numbers, which can be automatically determined from the contact stiffness matrix. For numerical solution of implicit equation (9), Uzawa's algorithm can be used, which leads to an iterative process involving one predictor–corrector step:

$$\text{predictor:} \quad \tau_n^{i+1} = r_n^i + \rho_n^i(x_n^i - \mu|\hat{\mathbf{u}}_t^i|); \quad \boldsymbol{\tau}_t^{i+1} = \mathbf{r}_t^i + \rho_t^i \mathbf{u}_t^i \tag{10}$$

$$\text{corrector:} \quad \mathbf{r}^{i+1} = \mathrm{proj}(\boldsymbol{\tau}^{i+1}, K_\mu) \tag{11}$$

The gist of the method is that the corrector can be analytically calculated and Eq. (11) can be explicitly written as

$$\begin{aligned}
&\text{if } \mu|\boldsymbol{\tau}_t^{i+1}| < -\tau_n^{i+1} \text{ then } \mathbf{r}^{i+1} = 0 \quad \text{! no contact} \\
&\text{else if } |\boldsymbol{\tau}_t^{i+1}| \leqslant \mu\tau_n^{i+1} \text{ then } \mathbf{r}^{i+1} = \boldsymbol{\tau}^{i+1} \quad \text{! sticking} \\
&\text{else } \mathbf{r}^{i+1} = \boldsymbol{\tau}^{i+1} - \frac{(|\boldsymbol{\tau}_{t^{i+1}}| - \mu\tau_{n^{i+1}})}{(1+\mu^2)}\left(\frac{\boldsymbol{\tau}_t^{i+1}}{|\boldsymbol{\tau}_t^{i+1}|} + \mu\mathbf{n}\right) \quad \text{! sliding}
\end{aligned} \tag{12}$$

It is important to emphasis on the fact that this explicit formula is valid for both 2D and 3D contact problems with Coulomb's friction and allows us to obtain very stable and accurate results.

3. Hyperelastic bodies undergoing large deformations

Rubber or other polymer materials are said to be hyperelastic. Usually, these kind of materials undergo large deformations. In order to describe the geometrical transformation problems, the deformation gradient tensor is introduced by

$$\mathbf{F}_{ij}(\mathbf{x}) = \boldsymbol{\delta}_{ij} + \frac{\partial \mathbf{u}_i}{\partial \mathbf{x}_j} \quad \text{or} \quad \mathbf{F} = \mathbf{I} + \nabla\mathbf{u} \tag{13}$$

where $\mathbf{I}$ is the unity tensor, $\mathbf{x}$ the position vector and $\mathbf{u}$ the displacement vector.

Because of large displacements and rotations, Green–Lagrangian strain is adopted for the nonlinear relationships between strains and displacements. We note $\mathbf{C}$ the stretch tensor or the right Cauchy–Green deformation tensor ($\mathbf{C} = \mathbf{F}^{\mathrm{T}}\mathbf{F}$). The Green–Lagrangian strain tensor $\mathbf{E}$ is defined by

$$\mathbf{E} = (\mathbf{C} - \mathbf{I})/2 \tag{14}$$

In the case of hyperelastic law, there exists an elastic potential function W (or strain energy density function) which is a scale function of one of the strain tensors, whose derivative with respect to a strain component determines the corresponding stress component. This can be expressed by

$$S_{ij} = \frac{\partial W}{\partial \mathbf{E}_{ij}} = 2\frac{\partial W}{\partial \mathbf{C}_{ij}} \tag{15}$$

where $\mathbf{S}$ is the second Piola–Kirchoff stress tensor. In the particular case of isotropic hyperelasticity [26], Eq. (15) can be written by

$$S = 2\left[I_3 \frac{\partial W}{\partial I_3} C^{-1} + \left(\frac{\partial W}{\partial I_1} + I_1 \frac{\partial W}{\partial I_2}\right) I - \frac{\partial W}{\partial I_2} C\right] \tag{16}$$

where I_i ($i = 1, 2, 3$) denote the invariants of the right Cauchy–Green deformation tensor $\mathbf{C}$:

$$I_1 = \mathbf{C}_{ii}; \quad I_2 = (I_1^2 - \mathbf{C}_{ij}\mathbf{C}_{ij})/2; \quad I_3 = \det(\mathbf{C}) \tag{17}$$

The Blatz–Ko constitutive law is used to model compressible foam-type polyurethane rubbers [27]. The strain energy density function is given as follows

$$W = \frac{G}{2}\left[\frac{I_2}{I_3} + 2\sqrt{I_3} - 5\right] \tag{18}$$

where G is the shear modulus. By deriving the energy density (18) with respect to the three invariants, we obtain

$$\frac{\partial W}{\partial I_1} = 0; \quad \frac{\partial W}{\partial I_2} = \frac{G}{2}\frac{1}{I_3}; \quad \frac{\partial W}{\partial I_3} = \frac{G}{2}\left[-\frac{I_2}{I_3} + \frac{1}{\sqrt{I_3}}\right] \tag{19}$$

Reporting the result in Eq. (16) gives

$$\mathbf{S} = G\mathbf{F}^{-1}\{\sqrt{I_3}\mathbf{I} - \mathbf{B}^{-1}\}\mathbf{F}^{-\mathrm{T}} \tag{20}$$

where $\mathbf{B} = \mathbf{F}\mathbf{F}^{\mathrm{T}}$ is the left Cauchy–Green deformation tensor associated to $\mathbf{F}$.

Noting $J = \sqrt{\mathbf{det}(2\mathbf{E} + \mathbf{I})}$, the tensor $\mathbf{S}$ can also be written in function of $\mathbf{E}$:

$$\mathbf{S}(\mathbf{E}) = G\left\{J(2\mathbf{E} + \mathbf{I})^{-1} - (2\mathbf{E} + \mathbf{I})^{-2}\right\} \tag{21}$$

The Cauchy stress (or true stress) tensor σ is calculated from the second Piola–Kirchoff stress tensor $\mathbf{S}$ as follows

$$\boldsymbol{\sigma} = \frac{1}{\det(\mathbf{F})}\mathbf{F}\mathbf{S}\mathbf{F}^{\mathrm{T}} \tag{22}$$

4. Finite element formulation of nonlinear structures

In the linear analysis, a linear relation is assumed between strains and displacements. However, if there are large displacements and strains, such as in the case of foam applications, the nonlinear relation between strains and displacements on one hand and between stresses and strains on the other hand cannot be ignored. Also, the equilibrium equation of internal and external forces should be considered in the deformed configuration. The geometrically nonlinear analysis may be described by using the total or the updated Lagrangian formulations. The total Lagrangian formulation is derived with respect to the initial configuration. The updated Lagrangian formulation is derived with respect to the current configuration. In other words, the total Lagrangian formulation constructs the tangent stiffness matrix with respect to the initial configuration. On the other hand, the updated Lagrangian formulation constructs the tangent stiffness matrix with respect to the current configuration. The updated Lagrangian formulation is computationally effective [28] because it does not include the initial displacement matrix. In the total Lagrangian formulation, the initial configuration remains constant. This simplifies the computation [29]. Therefore, the total Lagrangian formulation was selected in this work for the finite element discretization.

According to Eqs. (13) and (14), the Green–Lagrangian strain includes formally linear and nonlinear terms in function of nodal displacements:

$$\mathbf{E} = (\mathbf{B}_{\mathrm{L}} + \mathbf{B}_{\mathrm{NL}}(\mathbf{u}))\mathbf{u} \tag{23}$$

where $\mathbf{B}_{\mathrm{L}}$ is the matrix which relates the linear strain term to the nodal displacements, and $\mathbf{B}_{\mathrm{NL}}(\mathbf{u})$, the matrix which relates the nonlinear strain term to the nodal displacements. From Eq. (23), the incremental form of the strain-displacement relationship is

$$\delta\mathbf{E} = (\mathbf{B}_{\mathrm{L}} + \mathbf{B}_{\mathrm{NL}}(\mathbf{u}))\delta\mathbf{u} \tag{24}$$

Using the principle of virtual displacement, the virtual work δW is given as

$$\delta W = \int_{V_0} \mathbf{S}\,\delta\mathbf{E}\,\mathrm{d}V - \mathbf{F}_{\mathrm{ext}}\,\delta\mathbf{u} - \mathbf{R}\,\delta\mathbf{u} \tag{25}$$

where V_0 is the volume of the initial configuration, $\mathbf{F}_{\mathrm{ext}}$, the vector of external loads and $\mathbf{R}$, the contact reaction vector.

From Eqs. (15)–(20), we obtain

$$\delta\mathbf{S} = \mathbf{D}\,\delta\mathbf{E} = \mathbf{D}(\mathbf{B}_{\mathrm{L}} + \mathbf{B}_{\mathrm{NL}}(\mathbf{u}))\delta\mathbf{u} \tag{26}$$

where $\mathbf{D}$ is the current stress–strain tensor which is obtained from the derivative of $\mathbf{S}$ with respect to $\mathbf{E}$ in Eq. (21):

$$\begin{aligned} D_{ijkl} = G\{&-2J(2\mathbf{E}+\mathbf{I})^{-1}_{ik}(2\mathbf{E}+\mathbf{I})^{-1}_{lj} + J(2\mathbf{E}+\mathbf{I})^{-1}_{lk}(2\mathbf{E}+\mathbf{I})^{-1}_{ij} \\ &+ 2[(2\mathbf{E}+\mathbf{I})^{-1}_{ik}(2\mathbf{E}+\mathbf{I})^{-2}_{lj} + (2\mathbf{E}+\mathbf{I})^{-2}_{ik}(2\mathbf{E}+\mathbf{I})^{-1}_{lj}]\} \end{aligned} \tag{27}$$

Substituting $\delta\mathbf{E}$ from Eq. (24) into Eq. (25) results in

$$\delta W = \int_{V_0} \mathbf{S}(\mathbf{B}_{\mathrm{L}} + \mathbf{B}_{\mathrm{NL}}(\mathbf{u}))\delta\mathbf{u}\,\mathrm{d}V - \mathbf{F}_{\mathrm{ext}}\,\delta\mathbf{u} - \mathbf{R}\,\delta\mathbf{u} = (\mathbf{F}_{\mathrm{int}} - \mathbf{F}_{\mathrm{ext}} - \mathbf{R})\delta\mathbf{u} \tag{28}$$

where the vector of internal forces is defined by

$$\mathbf{F}_{\mathrm{int}} = \int_{V_0} \mathbf{S}(\mathbf{B}_{\mathrm{L}} + \mathbf{B}_{\mathrm{NL}}(\mathbf{u}))\mathrm{d}V \tag{29}$$

Since $\delta\mathbf{u}$ is arbitrary, a set of nonlinear equations can be obtained as

$$\mathbf{F}_{\mathrm{int}} - \mathbf{F}_{\mathrm{ext}} - \mathbf{R} = 0 \tag{30}$$

This equation is strongly nonlinear, because of finite strains and large displacements of solid, as we can see from above sections. Besides, the constitutive law of contact with friction is usually represented by inequalities and the contact potential is even nondifferentiable. Instead of solving Eq. (30) in consideration of all nonlinearities at the same time, we propose a approach to separate the nonlinearities in order to overcome the complexness of calculation and to improve the numerical stability. A typical solution procedure for this type of nonlinear analysis is obtained by using the Newton–Raphson iterative procedure [30,31]:

$$\begin{cases} \mathbf{K}_{\mathrm{T}}^{i}\,\Delta\mathbf{u} = \mathbf{F}_{\mathrm{ext}} + \mathbf{R} - \mathbf{F}_{\mathrm{int}}^{i} \\ \mathbf{u}^{i+1} = \mathbf{u}^{i} + \Delta\mathbf{u} \end{cases} \tag{31}$$

where i and $i+1$ are the iteration numbers at which the equations are computed. $\mathbf{K}_{\mathrm{T}}^{i}$ is the tangent stiffness matrix, $\mathbf{u}$, the vector of nodal displacements, $\Delta\mathbf{u}$, the vector of nodal displacements correction, and $\mathbf{F}_{\mathrm{int}}^{i}$, the vector of internal forces. Taking the derivative of $\mathbf{F}_{\mathrm{int}}$ with respect to the nodal displacements $\mathbf{u}$ gives the tangent stiffness matrix as

$$\mathbf{K}_{\mathrm{T}} = \frac{\partial\mathbf{F}_{\mathrm{int}}}{\partial\mathbf{u}} = \int_{V_0} \left(\frac{\partial\mathbf{S}}{\partial\mathbf{u}}(\mathbf{B}_{\mathrm{L}} + \mathbf{B}_{\mathrm{NL}}(\mathbf{u})) + \mathbf{S}\frac{\partial\mathbf{B}_{\mathrm{NL}}(\mathbf{u})}{\partial\mathbf{u}} \right) \mathrm{d}V \tag{32}$$

In addition, by using Eq. (26), this expression can be written by

$$\begin{aligned} \mathbf{K}_{\mathrm{T}} &= \int_{V_0} \mathbf{B}_{\mathrm{L}}^{\mathrm{T}}\mathbf{D}\mathbf{B}_{\mathrm{L}}\,\mathrm{d}V_0 + \int_{V_0} \mathbf{S}\frac{\partial\mathbf{B}_{\mathrm{NL}}(\mathbf{u})}{\partial\mathbf{u}}\,\mathrm{d}V + \int_{V_0} (\mathbf{B}_{\mathrm{L}}^{\mathrm{T}}\mathbf{D}\mathbf{B}_{\mathrm{NL}} + \mathbf{B}_{\mathrm{NL}}^{\mathrm{T}}\mathbf{D}\mathbf{B}_{\mathrm{L}} + \mathbf{B}_{\mathrm{NL}}^{\mathrm{T}}\mathbf{D}\mathbf{B}_{\mathrm{NL}})\,\mathrm{d}V \\ &= \mathbf{K}_{\mathrm{E}} + \mathbf{K}_{\sigma} + \mathbf{K}_{\mathrm{U}} \end{aligned} \tag{33}$$

In Eq. (33), the first term is the elastic stiffness matrix $\mathbf{K}_{\mathrm{E}}$, the second term is the geometric stiffness (or initial stress stiffness) matrix $\mathbf{K}_{\sigma}$, and the third term is the initial displacement stiffness matrix $\mathbf{K}_{\mathrm{U}}$.

It is noted that Eq. (31) can not be solved directly because $\Delta\mathbf{u}$ and $\mathbf{R}$ are both unknown. The key idea is to determine the reaction vector $\mathbf{R}$ by Eqs. (10)–(12) in a reduced system which only concerns the contact nodes. Then the displacement increments $\Delta\mathbf{u}$ can be computed in the whole

structure, using contact reactions as external loading. The Newton–Raphson iterative solution procedure involving contact modeling is written as in Box 1.

Box 1. Newton–Raphson iterative solution procedure

1. Read the data: mesh, material properties, boundary conditions, ...
2. For each load step
   2.1. Determine the external force vector $\mathbf{F}_{ext}$
   2.2. Detect contact conditions (local frame, gap vector...)
   2.3. For each Newton–Raphson equilibrium iteration
      2.3.1. Compute the tangent stiffness matrix $\mathbf{K}_T$ and the internal force vector $\mathbf{F}_{int}$
      2.3.2. Modify $\mathbf{K}_T$ and $\mathbf{F}_{int}$ for essential boundary conditions
      2.3.3. Solve $\mathbf{K}_T\Delta\mathbf{u} = \mathbf{F}_{ext} - \mathbf{F}_{int}$
      2.3.4. Compute reaction forces $\mathbf{R}$ by local algorithm
      2.3.5. Solve $\mathbf{K}_T\,\Delta\mathbf{u} = \mathbf{F}_{ext} - \mathbf{F}_{int} + \mathbf{R}$
      2.3.6. Actualize $\mathbf{u} = \mathbf{u} + \Delta\mathbf{u}$
      2.3.7. Check convergence criteria, if not met, go to 2.3.1
   2.4. Gather element nodal displacement
   2.5. Compute stresses and strains for each element and output
3. Update step count, if simulation not complete, go to 2

5. Numerical examples

The corresponding algorithms are implemented in the finite element software FER/Contact [32]. In order to validate the developed numerical models, we propose to study two quite different plane strain geometries. It is noted that these analyses were performed on a PC (Pentium 4/2.8 GHz). To show the performance of the present approach, we give the CPU time which is respectively 30 s for the first example and 42 for the second one.

Example 1. Contact between a rigid body and a hyperelastic body with small slip

The first example studied concerns the indentation of a circular rigid cylinder into an hyperelastic body undergoing large deformations but with relatively small slip, as shown in Fig. 2. The radius of cylinder is $R = 50$ mm. The dimension of the deformable body is: $a = 280$ mm, $b = 80$ mm. The shear modulus of the material model is G = 10 MPa. The finite element discretization includes 444 four-node isoparametric plane strain elements and 502 nodes. Fifty load steps are performed for this problem and a vertical displacement of 1 mm is applied to the cylinder each step. Fig. 3 shows the computed deformed configuration for a friction coefficient $\mu = 0.4$, when the applied displacement is equal to 50 mm. In order to check the influence of friction effects on the applied load, a friction coefficient $\mu = 0.0$ is also used. Fig. 2 gives the evolution of applied load with respect to the controlled displacement of the cylinder. The influence of friction effects is obvious, only after 30 load steps.

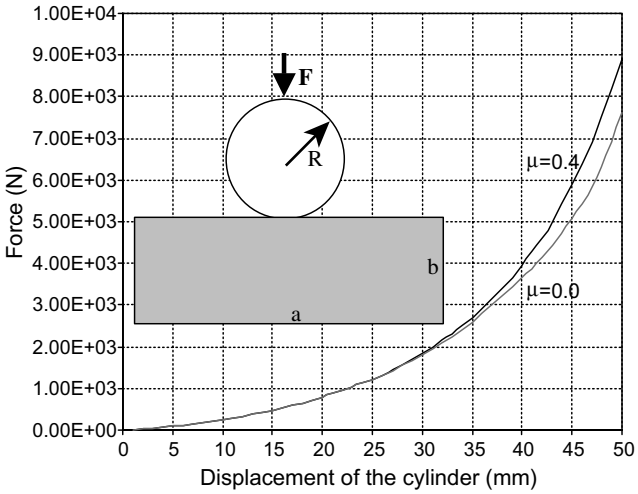

Fig. 2. Problem scheme and load–displacement curve.

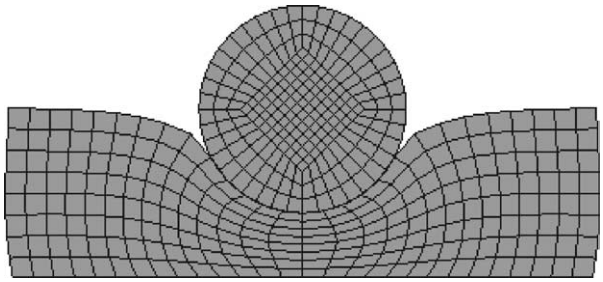

Fig. 3. Deformed shape ($\mu = 0.4$).

Example 2. Contact between two hyperelastic bodies with large slip

The second example simulates the contact between two hyperelastic bodies with large slip. The problem is displayed in Fig. 4.

The upper surface EF of Body 1 is given a rigid motion described by (**a**, **b**). The lower surface AC comes into contact with the upper surface IJ of Body 2. The characteristics of this example are:

- Geometric sizes: AC = CE = EF = FA = IH = JG = 500 mm; IJ = HG = 1500 mm
- Shear modulus: $G_1 = 5000$ MPa, $G_2 = 2500$ MPa
- Friction coefficient: $\mu = 0.2$
- Boundary conditions: $|\mathbf{a}| = 60$ mm, $|\mathbf{b}| = 400$ mm on EF, Displacements imposed to zero on GH.

The finite element discretization includes 108 eight-node isoparametric plane strain elements and 386 nodes. Each element has nine integration points. The number of load steps performed for

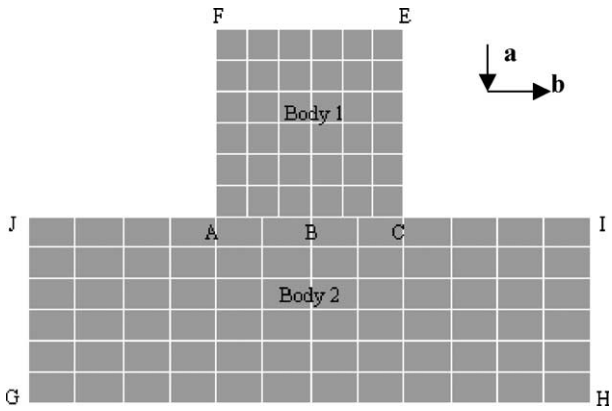

Fig. 4. Contact between two hyperelastic bodies under displacement control.

this example is respectively 20 and 180 for application of **a** and **b**. Figs. 5 and 6 show the deformed meshes for each deformation scenario. Figs. 7 and 8 show respectively the variation of normal and

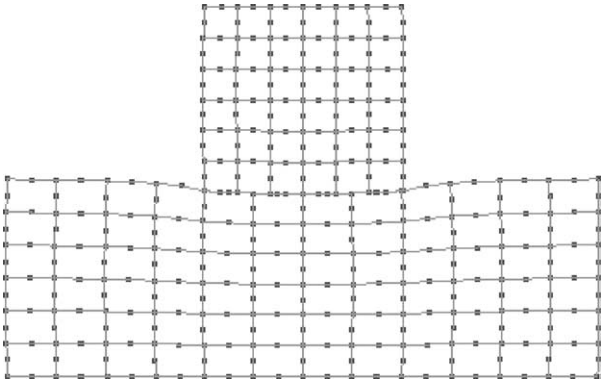

Fig. 5. Deformed meshes after application of **a**.

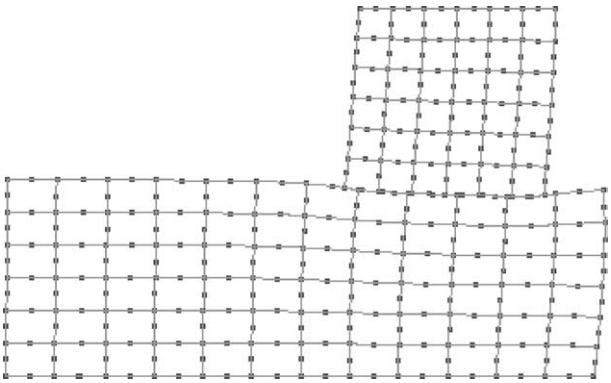

Fig. 6. Deformed meshes after application of **a** and **b**.

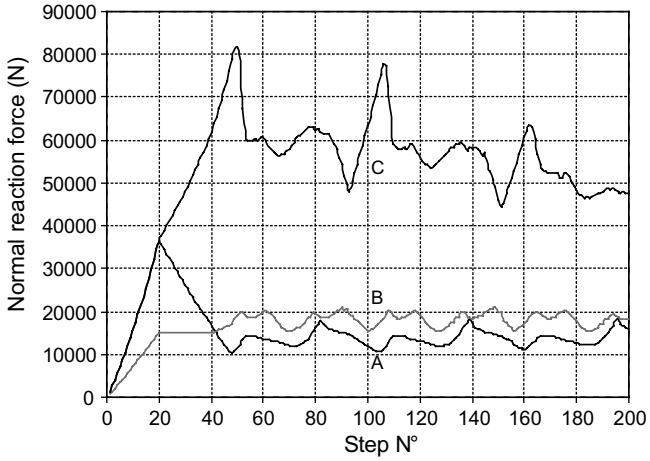

Fig. 7. Variation of normal contact forces vs. load steps.

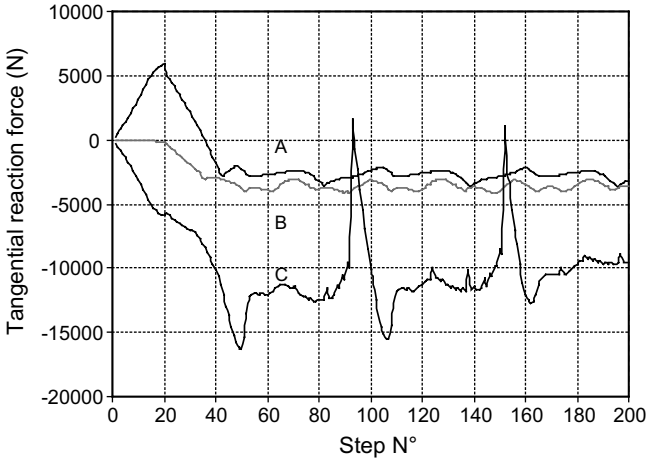

Fig. 8. Variation of tangential contact forces vs. load steps.

tangential contact forces on three selected points A, B and C (see Fig. 4). Fig. 9 gives the ratio of contact forces from which we can observe the evolution of contact states (sticking or sliding) on different points.

6. Conclusions

The main purpose of this paper is to present a finite element solution of large deformation contact problems with Coulomb friction between two hyperelastic bodies. This problem includes multiples nonlinearities: geometrical, material and frictional contact. The above numerical results demonstrate that the proposed algorithms, for the local analysis of frictional contact problems

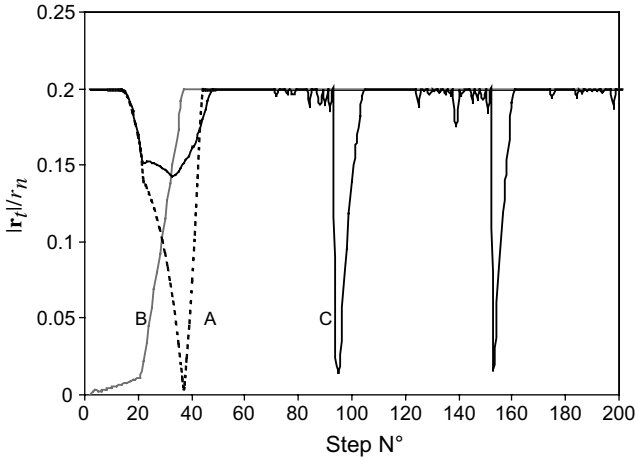

Fig. 9. Evolution of contact states vs. load steps.

and for the global resolution of nonlinear equation, are capable of handling a wide range of engineering applications. These include frictional contact between deformable or rigid bodies with small or large tangential slip. The constitutive law of deformable bodies can be linear elastic or nonlinear hyperelastic in the framework of large deformations and large displacements.

References

[1] S.H. Chan, I.S. Tuba, A finite element method for contact problems of solid bodies, Int. J. Mech. Sci. 13 (1971) 615–639.
[2] B. Fredriksson, Finite element solution of surface non-linearities in structural mechanics with special emphasis to contact and fracture mechanics problems, Comput. Struct. 6 (1976) 281–290.
[3] N. Kikuchi, J.T. Oden, Contact problems in elastostatics, in: J.T. Oden, G.F. Carey (Eds.), Finite Elements, vol. 5, Prentice-Hall, Englewood Cliffs, NJ, 1984.
[4] ANSYS Theory Reference, Release 5.6, 1999.
[5] A. Francavilla, O.C. Zienkiewicz, A note on numerical computation of elastic contact problems, Int. J. Numer. Methods Eng. 9 (1975) 913–924.
[6] T.D. Sachdeva, C.V. Ramarkrishnan, A finite element solution for the two-dimensional elastic contact problems with friction, Int. J. Numer. Methods Eng. 17 (1981) 1257–1271.
[7] D.H. Nguyen, G. De Saxcé, Frictionless contact of elastic bodies by finite element method and mathematical programming technique, Comput. Struct. 11 (1980) 55–67.
[8] A. Klarbring, G. Björkman, A mathematical programming approach to contact problems with friction and varying contact surface, Comput. Struct. 30 (1988) 1185–1198.
[9] W.X. Zhong, S.M. Sun, A parametric quadratic programming approach to elastic contact problems with friction, Comput. Struct. 32 (1989) 37–43.
[10] K.J. Bathe, A. Chaudhary, A solution method for planar and axisymmetric contact problems, Int. J. Numer. Methods Eng. 21 (1985) 65–88.
[11] B. Nour-Omid, P. Wriggers, A two-level iteration method for solution of contact problems, Comput. Methods Appl. Mech. Eng. 54 (1986) 131–144.
[12] M. Jean, G. Touzot, Implementation of unilateral contact and dry friction in computer codes dealing with large deformation problems, J. Theor. Appl. Mech. 7 (1988) 145–160.

[13] P. Alart, A. Curnier, A mixed formulation for frictional contact problems prone to Newton like solution methods, Comput. Methods Appl. Mech. Eng. 92 (1991) 353–375.
[14] J.C. Simo, T.A. Laursen, An augmented Lagrangian treatment of contact problems involving friction, Comput. Struct. 42 (1992) 97–116.
[15] A. Klarbring, Mathematical programming and augmented Lagrangian methods for frictional contact problems, in: A. Curnier (Ed.), Proc. Contact Mechanics Int. Symp., PPUR, 1992, pp. 369–390.
[16] J.H. Heegaard, A. Curnier, An augmented Lagrangian method for discrete large slip problems, Int. J. Numer. Methods Eng. 36 (1993) 569–593.
[17] G. De Saxcé, Z.Q. Feng, New inequality and functional for contact with friction: The implicit standard material approach, Mech. Struct. Mach. 19 (1991) 301–325.
[18] Z.H. Zhong, Finite Element Procedures for Contact–impact Problems, Oxford University Press, Oxford, 1993.
[19] P. Wriggers, Computational Contact Mechanics, John Wiley & Sons, 2002.
[20] A. Curnier, Q.C. He, A. Klarbring, Continuum mechanics modelling of large deformation contact with friction, in: M. Raous, M. Jean, J.J. Morau (Eds.), Contact Mechanics, Plenum, New York, 1995, pp. 145–158.
[21] G. Pietrzak, A. Curnier, Large deformation frictional contact mechanics: continuum formulation and augmented Lagrangian treatment, Comput. Methods Appl. Mech. Eng. 177 (1999) 351–381.
[22] A. Klarbring, Large displacement frictional contact: a continuum framework for finite element discretization, Eur. J. Mech. A/Solids 14 (1995) 237–253.
[23] Y.C. Wang, R. Lakes, Analytical parametric analysis of the contact problem of human buttocks and negative Poisson's ratio foam cushions, Int. J. Solids Struct. 39 (2002) 4825–4838.
[24] A.S. Bretelle, M. Cocou, Y. Monerie, Unilateral contact with adhesion and friction between two hyperelastic bodies, Int. J. Eng. Sci. 39 (2001) 2015–2032.
[25] G. De Saxcé, Z.Q. Feng, The bipotential method: a constructive approach to design the complete contact law with friction and improved numerical algorithms, in: Recent Advances in Contact Mechanics, Int. J. Math. Comput. Model. 28 (4–8) (1998) 225–245 (special issue).
[26] P.G. Ciarlet, Elasticité Tridimensionnelle, Masson, Collection RMA, 1985.
[27] P.J. Blatz, W.L. Ko, Application of finite elastic theory to the deformation of rubbery materials, Trans. Soc. Rheol. 6 (1962) 223–251.
[28] O.C. Zienkiewicz, R.L. Taylor, in: The Finite Element Method, fourth ed., vol. 2, McGraw-Hill, Berkshire, UK, 1991.
[29] M.A. Crisfield, Non-linear Finite Element Analysis of Solid and Structures, Wiley, Chichester, UK, 1991.
[30] T. Belytschko, W.K. Liu, B. Moran, Nonlinear Finite Elements for Continua and Structures, Wiley, Chichester, UK, 2000.
[31] J.C. Simo, T.J.R. Hughes, Computational Inelasticity, Springer-Verlag, New York, 1998.
[32] Available from <http://gmfe16.cemif.univ-evry.fr:8080/~feng/Fercontact.html>.